Alumina–aluminum interpenetrating-phase composites with three-dimensional periodic architecture

C. San Marchi [a,*], M. Kouzeli [a,b], R. Rao [c], J.A. Lewis [c], D.C. Dunand [a]

[a] *Department of Materials Science and Engineering, Northwestern University, Evanston, IL 60208, USA*
[b] *Magnetic Resonance Science Center, University of California, San Francisco, CA 94143, USA*
[c] *Department of Materials Science and Engineering, University of Illinois, Urbana, IL 61801, USA*

Abstract

Robotic deposition was used to create an alumina structure with three-dimensional periodicity and submillimeter feature size. Liquid metal infiltration of this structure resulted in an Al_2O_3–Al interpenetrating-phase composite exhibiting low thermal expansion and high compressive strength.
© 2003 Acta Materialia Inc. Published by Elsevier Ltd. All rights reserved.

1. Introduction

Interpenetrating phase composites (IPCs) represent a family of materials whose microstructure is characterized by the continuity and interpenetration of two or more phases. In the context of ceramic–metal IPCs, much of the driving force for investigating interpenetrating microstructures has been the toughening of ceramics by addition of low concentrations of a metal phase; therefore, IPCs of 60 vol.% ceramic or more are most common in the literature. The Al_2O_3–Al system is one of the most studied ceramic–metal IPC systems.

Several processing strategies have been developed to produce these composites, including infiltration of porous Al_2O_3 preforms [1–3], reactive metal penetration [4] and displacement reactions [5,6]. Other processing routes may result in discontinuous or partially discontinuous phases (e.g., directed metal oxidation [7] and powder metallurgy of mixed powders). All Al_2O_3–Al IPCs produced by these processes have a random, usually isotropic, spatial distribution of phases.

New opportunities for creating ceramic–metal IPCs with a highly regular architecture and tailored properties exist through the recent development of solid freeform fabrication techniques. Complex three-dimensional (3-D) ceramic architectures can be fabricated in a layerwise manner by fused deposition [8,9] and direct-write methods [10–15]. Direct-write techniques, such as robocasting [11–13], ink-jet printing [14], and micro-pen writing

---

[*] Corresponding author. Address: Sandia National Laboratories, MS-9402 P.O. Box 969, Livermore, CA 94551, USA. Tel.: +1-925-294-4880; fax: +1-925-294-3410.
E-mail address: cwsanma@sandia.gov (C. San Marchi).

[15], involve layer-by-layer assembly of colloidal inks. The fabrication of 3-D periodic structures with spanning (unsupported) features place the most stringent demands on ink design [12,13]. In the present paper, we report on an interpenetrating Al_2O_3–Al composite produced by liquid metal infiltration of a 3-D periodic Al_2O_3 preform with spanning elements that was produced by robotic deposition.

2. Experimental procedures

2.1. Alumina tower fabrication

Al_2O_3 powder (AKP-15, Sumitomo Chemical Co., NY, with a specific surface area of 3.9 m²/g, density of 3.97 g/cm³, and mean particle size of 0.8 μm), and ZrO_2 powder (3Y-TZ, Tosoh Corp, Tokyo, Japan, with a specific surface area of 14.3 m²/g, density of 5.89 g/cm³, and mean particle size of 0.4 μm) were mixed with a volume ratio of 95:5. A 30 vol.% ceramic suspension was created by adding the mixed powders to a 40% aqueous solution of an ammonium polyacrylate polymer (Darvan 821A, from Vanderbilt Co, Norwalk, CT). This stable suspension was vigorously agitated for 1 h to ensure homogeneity and then centrifuged at 1500 rpm for 1 h. After centrifugation, the supernatant was removed to increase the solids loading to approximately 54 vol.%. Methylcellulose (Methocel F4M, from Dow Chemical, Midland, MI) was added (7 mg/ml of ceramic) as a viscosifying aid. Gelation was induced by first adding 1.5 M $AlCl_3$ and then lowering the pH via addition of 1 M HNO_3. The pH was adjusted to roughly 8.5 with 1 M HNO_3 and 1.5 M NH_4OH to achieve the desired equilibrium shear modulus G' of ∼1 MPa. The colloidal gel-based ink contained approximately 52 vol.% solids.

Two Al_2O_3 towers, consisting of 30 alternating 0/90 layers of parallel rods, were produced by robotic deposition using the gel-based ink described above. The ink delivery system was mounted on a z-axis motion control stage that prints onto a moving x–y stage. The entire process was controlled through a custom-designed, computer-aided, direct-write program (RoboCad 3.2). The deposition

nozzle (330 μm in diameter) was coated with non-wetting oil, which deposits onto the extruded ink filament to inhibit drying during the build sequence. After assembly, the 30-layer tower structures were dried in air for 24 h and then sintered in air at 1600 °C for 2.5 h. The final rod diameter was approximately 250 μm in the densified structures.

Fig. 1a is a top view of a sintered Al_2O_3 tower with nominal dimensions of $6 \times 4 \times 4$ mm³. Fig. 1b is a schematic illustrating how the tower was created. The first layer is composed of a series of equidistant rods parallel to the x-axis with "hairpins" connecting them. The second layer is identical to the first but rotated by 90°, i.e., parallel to the y-axis. Use of gel-based inks allows the deposited filamentary rods to maintain their shape without deformation as they span gaps between rods in underlying layers [12,13]. This process was repeated 15 times, resulting in a 30-layer tower structure with simple cubic symmetry. Fig. 2a and b are a side view and 3-D schematic of the tower
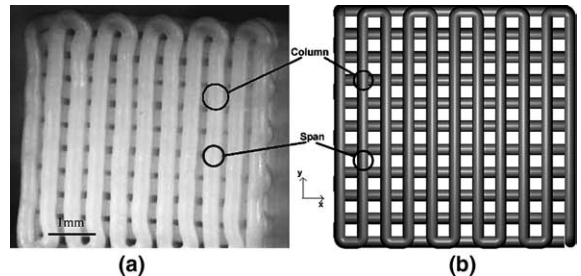

Fig. 1. (a) Top view of an alumina tower and (b) an idealized schematic illustrating the layering pattern.
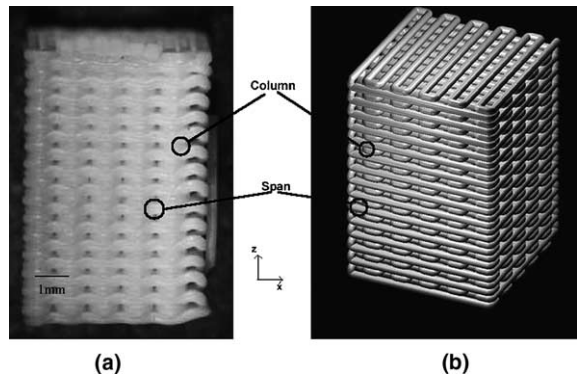

Fig. 2. (a) Side view of the tower architecture and (b) an idealized 3-D schematic.

architecture, respectively. The towers consist of vertical columns (parallel to the z-axis) and horizontal spans (parallel to the x- and y-axes). Vertical columns are formed at the interface between horizontal rods in one layer and those in the adjacent layers, as they partially fuse together during deposition [12]. The unsupported regions of the deposited rods form spans that connect columns together within the 3-D periodic Al_2O_3 tower.

2.2. Composite processing

Sintered Al_2O_3 towers were placed within cavities machined into a graphite block; the dimensions of each cavity were slightly larger than an individual tower (by about 1 mm on a side). The graphite block was placed within an alumina crucible and a rod of 99.99% pure aluminum was placed on top of the graphite. The crucible was put in a gas-pressure, liquid-metal infiltration apparatus [16] and heated under vacuum to a temperature of 750 °C. The liquid metal was infiltrated into the evacuated open volume of the tower under an argon pressure of 3.5 MPa and the resulting composite was directionally solidified. A skin of pure aluminum, nominally 0.5 mm in thickness, encapsulated the composite and was removed from the two 4×4 mm^2 sides by light mechanical polishing to ensure uniform loading during subsequent mechanical testing. This skin was retained on the other four (4×6 mm^2) sides to prevent mechanically damaging the Al_2O_3 architecture.

2.3. Property measurements

A calibrated horizontal push-rod dilatometer (Orton Model 1600, Westerville OH) was used to measure the thermal expansion of an Al_2O_3 tower and the Al_2O_3–Al composite in the z-direction by heating to 200 °C at a rate of 3 °C/min. After the dilatometric experiments, the compressive strength of both tower and composite was measured at constant crosshead speed, corresponding to a nominal strain rate of 10^{-3} s^{-1}. Both the Al_2O_3 tower and the Al_2O_3–Al composite were loaded in the z-direction, so that the columns created at the contact points between layers were parallel to the loading direction. The compression platens were

lubricated with Teflon and two methods were used to determine the strain in the sample: laser extensometry and the crosshead motion corrected for the compliance of the testing machine. Neither method produced data with sufficient resolution for stiffness determination.

3. Results and discussion

The density of the fired elements in the Al_2O_3 towers was determined by helium pycnometry to be 3.7 g/cm^3, which was lower than expected for a dense mixture of Al_2O_3–5 vol.% ZrO_2 (4.07 g/cm^3 estimated from rule of mixtures). This value corresponds to a closed porosity of as much as 9% within the ceramic that cannot be infiltrated (subsequently fabricated towers exhibit densities greater than 95% of theoretical). The overall density of the towers was estimated from their mass and dimensions as 2.6 g/cm^3; the volume fraction of ceramic in the tower is then calculated as 70%. The density of the Al_2O_3–Al composite was measured as 3.4 g/cm^3 by helium pycnometry (this value is corrected for the Al skin, by subtracting its contribution based on the dimensions of the composite compared to those of the tower before infiltration). Using the density of Al (2.69 g/cm^3), the ceramic (3.7 g/cm^3) and the composite (3.4 g/cm^3), the concentration of Al_2O_3 in the composite is calculated to be 70 vol.%. The good agreement with the previous value of 70 vol.% indicates that infiltration was complete and that all open porosity in the tower was filled with Al.

3.1. Thermal expansion

The average coefficient of thermal expansion (CTE) of the as-sintered Al_2O_3 tower between 50 and 200 °C is $6.7 \pm 0.7 \times 10^{-6}$ K^{-1}, as measured by dilatometry (near room temperature, the CTE of the tower is about 6×10^{-6} K^{-1}). This value is consistent with CTE reported for bulk Al_2O_3 in this temperature range (5–7×10^{-6} K^{-1} [1,17]). The CTE of the Al_2O_3–Al composite was measured to be $8.9 \pm 0.3 \times 10^{-6}$ K^{-1} between 50 and 200 °C.

Plasticity during thermal expansion, which tends to increase the CTE value as compared to

elastic predictions [18], is not relevant here, because the relatively small temperature excursion ($\Delta T = 175$ °C) results in a representative mismatch strain $\Delta \alpha \, \Delta T$ of only about 0.4%. Assuming that, upon cooling from the processing temperature, the matrix had reached its yield stress in tension and was work-hardened, this small mismatch strain during CTE measurement is unlikely to induce significant plasticity, so that modeling the elastic interaction of the constituents should provide reasonable predictions for thermal expansion.

Analytical solutions for the CTE of isotropic discontinuously reinforced composites (DRCs) have been developed by considering the thermal elastic interactions of an inclusion surrounded by matrix in specific volumetric proportions (see review in Ref. [19]). Two limits can be identified depending on which phase is the inclusion. These bounds are often referred to as the Kerner (upper) bound and the Schapery (lower) bound. The upper bound for the CTE represents the metal matrix composite configuration, i.e., in the context of this study, Al_2O_3 particles in a continuous Al matrix. The ceramic matrix configuration, with Al inclusions in an Al_2O_3 matrix, is captured by the lower bound, where the continuous Al_2O_3 matrix significantly constrains the expansion of the discontinuous metal.

Although these inclusion models do not reflect the interpenetrating microstructure of an IPC, a solution for the CTE of an interpenetrating microstructure can be obtained by self-consistently solving the equations for the two bounding geometries [20], the so-called classical self-consistent (CSC) approach. This solution, as well as numerical solutions [21,22], fall within the elastic bounds and are typically close to the lower elastic bound (i.e., near the solution for a ceramic matrix composite). Using the material properties listed in Table 1, the upper and lower elastic bounds are calculated to be 10.8 and 9.2×10^{-6} K^{-1} respectively. The measured CTE (8.9×10^{-6} K^{-1}) is, within experimental error, equal to the lower elastic limit, as anticipated since the alumina is continuous. Other researchers have reported the CTE of IPCs with 70 ± 5 vol.% Al_2O_3 to be closer to the upper bound, around 10×10^{-6} K^{-1} [1,5,6]; exact comparison is

Table 1
Properties of pure aluminum and alumina, average between 50 and 200 °C

	Al	Al_2O_3
Young's modulus, E (GPa)	63.5[a]	410 [17]
Poisson's ratio ($v-$)	0.35	0.235[a]
Shear modulus, G (GPa)	23.5 [28]	166 [17]
Bulk modulus, K (GPa)	70.6[a]	258[a]
CTE ($\alpha \times 10^{-6}$ K^{-1})	24.8 [29]	6.2 [17]

[a] Determined from elastic relationships: $G = E/(2 + 2v)$; $K = E/(3 - 6v)$.

not possible since the CTE was not reported in the same temperature range.

Metal–ceramic composites are used for thermal management applications, such as electronic packaging, where CTE values close to silicon (4.1×10^{-6} K^{-1}) and alumina (6.7×10^{-6} K^{-1}) are desired, coupled with thermal conductivities approaching that of aluminum alloys [23]. Although the thermal conductivity of the present infiltrated tower was not measured, the use of high purity aluminum, the coarse size of the constituents and the spatial periodicity of the composite (the Al "columns" in the composite act as "heat pipes"), all point towards improved thermal conductivity as compared to IPCs described in the literature, which typically exhibit an alloyed aluminum, smaller architectural size scales and a random distribution of the constituents.

3.2. Mechanical properties

The compressive strength of the Al_2O_3 tower was measured as 190 MPa, which is low compared to typical values for dense Al_2O_3 (2.5–3.8 GPa), but similar to tensile and flexure strengths for bulk Al_2O_3 (250 and 400 MPa respectively [17]). Fracture stresses measured in four-point bending have been reported in the range 140 and 200 MPa for porous Al_2O_3 preforms with 70 ± 5 vol.% Al_2O_3 prepared for subsequent infiltration to produce IPCs [2,3]. Periodic alumina and mullite structures (70 vol.%) produced by fused deposition, however, have compression strengths that are less than 50 MPa [9,24]. Finite-element modeling of those periodic mullite structures shows that the continuous

columnar elements support the applied compressive loads [25] while the spans are in tension, as they prevent buckling of the columns. Since alumina is nearly an order of magnitude stronger in compression than tension, failure is expected in the spans loaded in tension, resulting in spallation of layers parallel to the loading direction, as reported for the periodic mullite structures [25]. The same failure mechanism was observed in the present investigation, indicating that the majority of the microstructural damage was indeed generated in the horizontal spans. Sharp corners at the junctions between columns and spans are likely to initiate this failure at relatively low tensile stresses; failure stresses may also be lowered by porosity in the ceramic. This interpretation implies that failure of the tower is determined by the defects within the spans, not by the columns or the span lengths. We note that standard ceramic foam models [26] assume that all spans have a large length-to-thickness ratio, so that bending failure predominates; this assumption is not appropriate for the present towers.

The compressive strength (failure stress) of the composite was 700 MPa, an improvement by a factor of almost 4 over the un-infiltrated tower. It is unlikely that this improvement is due to a fourfold decrease in the load carried by the ceramic phase through load transfer to aluminum, given its much lower strength and stiffness as compared to alumina. Rather, the main effect of the metallic phase may be similar to that of the horizontal alumina spans: prevention of buckling in the load-bearing alumina columns (similarly, in unidirectional fiber composites tested in compression, all of the buckling resistance is supplied by the matrix). Metallographic observation of the deformed composite revealed that damage developed in a similar manner as in the unreinforced tower: failure occurred predominantly in the spans near the corners where the spans join the columns, Fig. 3a. As the spans fractured, the aluminum phase not only carries an increasing proportion of the transverse tensile stresses but also blunts cracks by plastic deformation, preventing catastrophic propagation of cracks within the alumina phase. On a macroscopic level, damage in the composite was found to link into a macroscopic
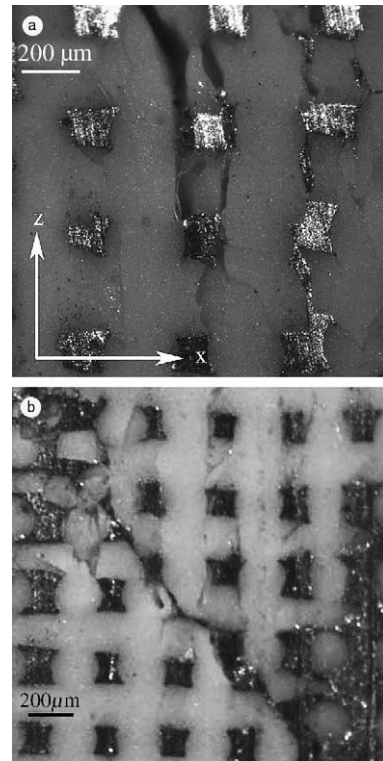

Fig. 3. Optical micrographs of the composite sectioned after compressive failure parallel to the loading direction (vertical) showing (a) fracture of spanning elements (note some aluminum has been smeared into cracks in the alumina due to sectioning); and (b) the macroscopic crack at 45° to the loading axis. Note also the continuous nature of the vertical columns, which were created due to fusion of the deposited rods at their contact points.

crack forming at an angle of about 45° with respect to the applied load, i.e., on the plane of maximal shear stress, as typically observed for brittle materials in compression, Fig. 3b.

Higher compressive strengths have been reported for Al_2O_3–Al IPCs produced by displacement reactions [5] (up to 1200 MPa for 64 vol.% Al_2O_3 [6]). Numerous authors have reported bending strengths between 400 and 700 MPa for 65–75 vol.% Al_2O_3–Al IPCs [2–5], implying compressive strengths of 700 MPa or greater. Those materials, however, have a much finer microstructure corresponding to smaller flaw size, and thus higher strength in the ceramic. The strength of sintered alumina is also dependent on

the sintering conditions and additives, making direct comparison difficult without detailed analysis of the sintered microstructure. The aluminum matrix, in the case of material produced by displacement reactions, has significant (and difficult to control) amounts of silicon, compared to the high-purity aluminum used in this study, again appreciably affecting mechanical and thermal properties. Mechanical data for mullite-aluminum IPCs produced by a process analogous to the one used here (fused deposition of the mullite followed by infiltration with aluminum [27]) have not been reported, although as mentioned above, the un-infiltrated mullite preforms displayed a compressive strength much lower than in the present study.

4. Summary

An interpenetrating-phase composite with a 3-D periodic architecture was created by pressure infiltration of an alumina tower with liquid aluminum. The alumina tower with periodic cubic symmetry was produced by robotic deposition of an Al_2O_3-5 vol.% ZrO_2 gel. The composite, consisting of 70 vol.% ceramic, exhibits a low thermal expansion of 8.9×10^{-6} K^{-1}, close to the lower elastic (Schapery) bound for thermal expansion. The compressive strength of the composite is much greater than that of the un-infiltrated ceramic preform (700 versus 190 MPa), with only a small increase in density (3.4 versus 2.6 g/cm^3).

Acknowledgements

References

[1] Skirl S, Hoffman M, Bowman K, Wiederhorn S, Rodel J. Acta Mater 1998;46:2493.
[2] Prielipp H, Knechtel M, Claussen N, Streiffer SK, Mullejans H, Ruhle M, et al. Mater Sci Eng A 1995;197:19.
[3] Zimmermann A, Hoffman M, Emmel T, Gross D, Rodel J. Acta Mater 2001;49:3177.
[4] Ewsuk KG, Glass SJ, Loehman RE, Tomsia AP, Fahrenholtz WG. Metall Mater Trans 1996;27:2122.
[5] Breslin MC, Ringnalda J, Xu L, Fuller M, Seeger J, Daehn GS, et al. Mater Sci Eng A 1995;195:113.
[6] Liu W, Koster U. Mater Sci Eng A 1996;210:1.
[7] Urquhart AW. Mater Sci Eng A 1991;144:75.
[8] Bandyopadhyay A. Adv Eng Mater 1999;1:199.
[9] Bose S, Darsell J, Hosick HL, Yang L, Sarkar DK, Bandyopadhyay A. J Mater Sci-Mater Med 2002;13:23.
[10] Chrisey DB. Science 2000;289:879.
[11] Cesarano J, Calvert P. US Patent no. 6 027 326, 2000.
[12] Smay JE, Gratson GM, Shepherd RF, Cesarano J, Lewis JA. Adv Mater 2002;14:1279.
[13] Smay JE, Cesarano J, Lewis JA. Langmuir 2002;18:5429.
[14] Seerden KAM, Reis N, Evans JRG, Grant PS, Halloran JW, Derby B. J Am Ceram Soc 2001;84:2514.
[15] Morissette SL, Lewis JA, Clem PG, Cesarano J, Dimos DB. J Am Ceram Soc 2001;84:2462.
[16] Mortensen A. In: Kelly A, Zweben C, editors. Comprehensive composite materials. New York: Elsevier; 2000. p. 521.
[17] Munro RG. J Am Ceram Soc 1997;80:1919.
[18] Olsson M, Giannakopoulos AE, Suresh S. J Mech Phys Solids 1995;43:1639.
[19] Delannay F. In: Kelly A, Zweben C, editors. Comprehensive composite materials. New York: Elsevier; 2000. p. 341.
[20] Wilkinson DS, Wolfgang P, Oeschner M. Prog Mater Sci 2001;46:379.
[21] Wegner LD, Gibson LJ. Int J Mech Sci 2000;42:925.
[22] Shen YL. Mater Sci Eng A 1998;252:269.
[23] Zweben C. J Metals 1998;50(6):47.
[24] Atisivan R, Bose S, Bandyopadhyay A. J Am Ceram Soc 2001;84:221.
[25] Hattiangadi A, Bandyopadhyay A. J Am Ceram Soc 2000;83:2730.
[26] Gibson LJ, Ashby MF. Cellular solids—structure and properties. 2nd ed. Cambridge, UK: Cambridge University Press; 1997. p. 510.
[27] Soundararajan R, Kuhn G, Atisivan R, Bose S, Bandyopadhyay A. J Am Ceram Soc 2001;84:509.
[28] Frost HJ, Ashby MF. Deformation-mechanism maps. In: The plasticity and creep of metals and ceramics. Oxford: Pergamon Press; 1982.
[29] Alcoa. Alcoa Aluminum Handbook. Pittsburgh: Aluminum Company of America; 1962. p. 39.